DELOCALIZATION OF ELECTRONIC EXCITATIONS
IN DISORDERED MOLECULAR SYSTEMS

R.J. GULOTTY, C.A. WALSH, F.G. PATTERSON,
William L. WILSON and M.D. FAYER

Department of Chemistry, Stanford University, Stanford, CA 94305, USA

Picosecond photon echo experiments are used to examine the nature of the electronic states of interacting molecules in the mixed molecular crystal system, pentacene in p-terphenyl at 1.5 K. The onset of delocalization of the pentacene first singlet electronic excited state with increasing pentacene concentration is manifest in very fast photon echo decays. The concentration dependence of the echo decay rates accords with theoretical estimates.

1. Introduction

The nature of optically excited states of interacting molecules or atoms in solids has been a subject of great interest for many decades [1–3]. For pure crystals, it is well established that the eigenstates are collective, delocalized excitations of the crystal [3]. In the other limit, an extremely low concentration impurity has localized eigenstates whose properties are in part determined by non-resonant interactions with the environment provided by the host crystal [4–6]. In between these two limits, in an impurity concentration range in which impurity intermolecular interactions are not negligible, the question of the proper description of the electronic eigenstates remains open [7].

In an idealized system in which the randomly distributed guest molecules (impurities) have identical site energies (no inhomogeneity), and there are no thermal fluctuations (absolute zero temperature) even small dipole–dipole intermolecular interactions among the guest molecules should result in delocalization. However, in real crystals, impurity absorption spectra display inhomogeneous broadening. The static inhomogeneity in guest site energies breaks the perfect degeneracy among the interacting molecules. In addition, at any finite temperature, fluctuations in molecular positions and orientations result in fluctuations in both site energies and in the magnitudes of the intermolecular

interactions [8–11]. The question of delocalization depends on a complex interplay between the strengths of the intermolecular interactions which tend to delocalize an excitation and the static and dynamic variations in site energies and intermolecular interactions, which tend to localize an excitation.

In this paper we present a picosecond photon echo study of the states of interacting pentacene molecules randomly distributed in p-terphenyl host crystals. The pentacene molecules interact via a transition dipole–transition dipole interaction which has a $1/r^3$ distance dependence. It has been theoretically demonstrated that for systems with intermolecular interactions that fall off as $1/r^4$ or faster, an abrupt transition from localized to delocalized states should occur [12]. However, for dipole–dipole interactions among pentacene molecules, a continuous transition should occur. As the concentration is increased from the low-concentration limit, the electronic transitions become delocalized over increasingly large regions of the crystal.

In the absence of inhomogeneous broadening, the delocalized states would form an impurity band that is observable through changes in the optical absorption lineshape. However, in real systems, inhomogeneous broadening masks the lineshape changes. This has led a number of groups to theoretically consider the influence of delocalization on the photon echo observable. Warren and Zewail [13] obtained an expression

for the photon echo decay in the absence of inhomo-geneous broadening. Root and Skinner [7] (RS) also considered the zero inhomogeneous broadening case and obtained a more accurate result which is similar to the Warren and Zewail expression. Simultaneous with the Root and Skinner work, Loring, Andersen and Fayer [14] (LAF) considered the problem in a some-what broader context. For the case of zero inhomo-geneous broadening, LAF obtained a result identical to the RS calculation. The two groups used distinct theoretical approaches, adding support to the results of the calculations.

In the absence of inhomogeneous broadening, RS and LAF determined that the short-time behaviour of the photon echo goes as $1 - Ct$, where C is a con-stant. This is the short-time expansion of an expo-nential which led to an expression for T_2, the homo-geneous dephasing,

$$T_2^{-1} = 5.07 \, \mu^2 f / a^3 \hbar, \tag{1}$$

where μ is the molecules' transition dipole moment, a^3 is the volume per molecule in the unit cell and f is the fraction of lattice sites occupied by impurity molecules.

LAF also included various models of inhomo-geneous broadening in their calculations, i.e. they considered both diagonal and off-diagonal disorder. The inhomogeneous distribution of site energies was taken to be Gaussian. In one limit, LAF took the site energies and spatial positions of molecules to be un-correlated. They also considered a simple model of correlated site energies and spatial positions. In all cases in which there is not perfect correlation, i.e. interacting molecules are not necessarily degenerate, the photon echo decays were calculated to be highly non-exponential. Therefore the decays cannot be described in terms of a single parameter, T_2. The cal-culations with uncorrelated inhomogeneous broadening display a very fast initial drop in the photon echo in-tensity followed by a much slower decay. The extent of the initial fast drop is determined by the strength of the intermolecular interactions (concentration and transition dipole moment). The time regime of the crossover between the fast drop and the slower decay is determined by the width of the Gaussian inhomo-geneous line.

The theoretical calculations briefly described above provide a context in which to discuss the experimental

results presented below. None of the calculations in-clude the effects of phonon induced fluctuations in site energies or intermolecular interactions. While the calculations are approximate, they serve a useful guide to the understanding of the experiments.
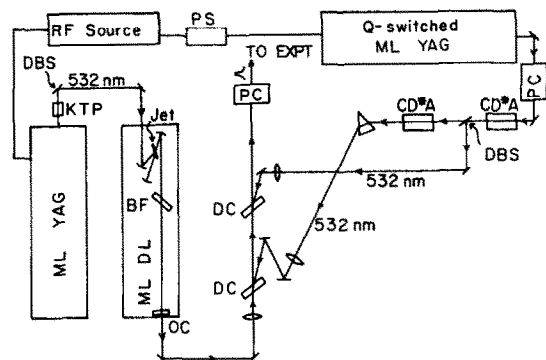
2. Experimental procedures

The theoretical calculations indicate that the fast decay of the photon echo intensity for a typical crystal will occur on an ≈ 100 ps timescale. In addition, theoretical considerations require the Rabi frequency ($\mu \cdot Et / \hbar$) to be large compared to the frequency spread of the impurity band levels. Thus, short, high-power pulses are required.

To obtain the necessary pulses, with high repetition rate and good shot-to-shot reproducibility, required for these non-linear experiments, a new type of am-plified picosecond laser system was employed (see fig. 1). A cw mode-locked Nd : YAG laser is used as the pump laser. The output consists of a stable ($\pm 2\%$) con-tinuous stream of ≈ 55 ps 1064 nm pulses separated by 12.4 ns. The average mode-locked power can be as high as 12 W TEM$_{00}$, but typically only 6 W was required. The 6 W output is focused onto a 5 mm long angle-tuned KTP doubling crystal, producing 400 mW of 40 ps, 5 nJ, 532 nm pulses (2.5 W of 532 nm has been obtained using the full 12 W of IR). This is used to pump a dye laser with an astigmatically compensated three-mirror folded optical cavity with a dye (Rhodamine 6G) jet. The tuning element used is a two-plate birefringent filter to achieve near trans-form limited pulses. The output of the dye laser con-sists of 70 mW, 1.75 ps pulses with a bandwidth of 3.5 Å.

The ≈ 1 nJ dye pulses are amplified with the frequency doubled output of a cw-pumped, Q-switched and mode-locked Nd : YAG laser at a 2/3 kHz rep-etition rate. The amplifying pulses are synchronized to the dye pulses by mode-locking both Nd : YAG lasers with the same crystal oscillators (hence the cavity lengths of both lasers are matched). Two am-plifying stages are used. A single 115 μJ IR pulse is selected by a Pockels cell from the amplifying laser pulse train and is frequency doubled with a CD*A angle-tuned doubling crystal to produce a 60 μJ, 532 nm single pulse. The remaining 20 μJ of undoubled

A. LASER SYSTEM

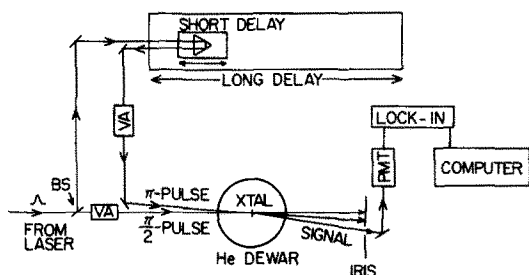## B. EXPERIMENTAL PHOTON ECHO SET-UP

Fig. 1. (A) Amplified cw mode-locked dye laser system. A cw mode-locked Nd : YAG laser synchronously pumps a mode-locked dye laser. The dye laser pulses are amplified with a Q-switched mode-locked Nd : YAG laser. The mode-lockers of the two Nd : YAG lasers are driven with the same rf source, so that all three lasers are synchronized and dye laser pulse amplification can be performed at high repetition rates. See section 2 for details. PS = phase shifter; PC = Pockels cell; DBS = dichroic beam splitter; DC = Brewster angle flowing dye cell; BF = birefringent filter; OC = output coupler. (B) Experimental photon echo apparatus. The single amplified dye laser pulse is split into two excitation pulses, which can be independently attenuated so that they can be accurately set to π and $\pi/2$ pulses. The π pulse is directed into a corner cube mounted on a motorized micrometer-driven translation stage. This allows up to 330 ps delay of the π pulse relative to the $\pi/2$ pulse. The translation stage itself sits on top of a motor-driven carriage on a precision optical rail, which allows up to 9 ns delay of the π pulse, without optical realignment. BS = beam splitter; VA = variable attenuator which consists of a polarizer—half-wave plate—polarizer sequence.

IR is separated from the green single pulse and passed through a second doubling crystal to produce ≈ 5 μJ in a second green single pulse. These two green pulses are used to pump the two amplifying stages. The dye

amplifiers consist of flowing Brewster angle dye (5 $\times$ 10^{-4} M Rhodamine B) cells with 1 mm optical path lengths using a slightly non-collinear pump geometry. The amplification is non-linear, resulting in a broadening of the pulse duration by a factor of ≈ 2. The amplified pulse is additionally isolated from the unamplified cw dye pulses using a Pockels cell (avalanche transistor driven) to give a $>10^6$ ratio of the single amplified pulse to the background pulses. The result is a very clean, single 4 ps, 2 μJ, 592 nm dye laser pulse at 2/3 kHz.

The single, amplified dye pulse is split into the π and $\pi/2$ pulses (see fig. 1). The π pulse is delayed relative to the $\pi/2$ pulse using a double motorized delay line. A corner cube sits on top of a motorized micrometer driven translation stage which provides 330 ps delay. The motorized micrometer translation stage itself sits on top of a carriage on a precision optical rail which is motor driven to provide a 9 ns delay. This double delay line allows measurement of both very fast and slower decays without any optical realignment. The intensities of both pulses can be varied independently and were set to π and $\pi/2$ by maximizing the photon echo signal from a low-concentration crystal. The $\pi/2$ and π pulses are crossed at a small angle in the sample. The echo signal propagates in a unique direction, and it is spatially isolated from the excitation pulses. The photon echo signal is detected by a cooled photomultiplier tube and a lock-in amplifier and recorded by computer.

In order to have samples with relatively low optical density yet sufficiently high concentration, it is necessary to have very thin crystals (1–10 μm). These thin, mixed molecular crystals were obtained by cosublimation of pentacene with p-terphenyl. Typical crystals are ≈ 5 μm thick with a concentration of $\approx 10^{-5}$ mole PC/mole PTP. The crystals were weighed on a microgram balance, and their area estimated using a microscope. From the density of p-terphenyl, the average thickness of the sample is determined. Since the concentration of pentacene in these samples is not macroscopically uniform, it is necessary to measure the concentration on the particular spot where the echo data are taken. The concentration of PC in the crystals is determined from the peak optical density, the fwhm of the absorption line, the sample thickness and the dipole moment of the $S_0 \rightarrow S_1$ pentacene transition.

3. Results and discussion

Fig. 2a presents photon echo decay data from the O_1, O_2 transitions of pentacene in p-terphenyl [15, 16] for a high-concentration crystal ($c = 8.8 \times 10^{-5}$ mole PC/mole PTP, thickness = 6 μm) and fig. 2b presents data for a low-concentration crystal ($c = 1.4 \times 10^{-6}$ mole PC/mole PTP, thickness = 450 μm). The high-concentration decay curve is highly non-ex-
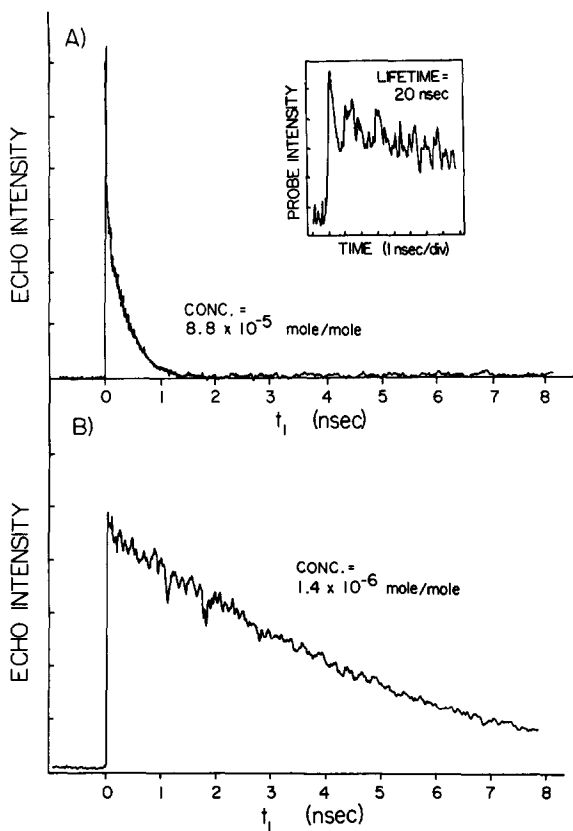

Fig. 2. (A) Photon echo decay for the O_1, O_2 transitions in pentacene in p-terphenyl for a high-concentration crystal ($c = 8.8 \times 10^{-5}$ mole PC/mole PTP). The decay curve can be represented as the sum of two exponentials with decay times $\tau_f = 16$ ps and $\tau_s = 330$ ps. The fast component is not resolved and appears as a spike at $t_1 = 0$. (B) Photon echo decay for a low-concentration crystal ($c = 1.4 \times 10^{-6}$ mole PC/mole PTP). The decay is a single exponential with decay time $\tau_{lc} = 4.5$ ns. The inset shows the result of a pump–probe experiment carried out on the high-concentration crystal. The measured decay time is 20 ± 3 ns, showing that population relaxation is not responsible for fast echo decay observed in the high-concentration crystal.

ponential. It can be approximately represented by the sum of two exponentials with decay times $\tau_f = 16$ ps, and $\tau_s = 330$ ps (f ≡ fast and s ≡ slow). The low-concentration crystal gives a single exponential decay with decay time $\tau_{lc} = 4.5$ ns. The low- and high-concentration decay curves were taken under identical experimental conditions. These data sets are typical of the dramatic differences observed in the photon echo decays as a function of concentration.

To ensure that delocalization is responsible for the fast high-concentration decays, two points must be addressed: optical density effects and population relaxation. It is well documented that in the low-concentration limit, samples with high optical density can yield anomalously fast decays [16]. At the temperature of these experiments, low concentration pentacene in p-terphenyl has $T_2 = 2T_1$ [9]. For the O_1, O_2 transition $T_2 = 44$ ns [9] and the echo signal decays with a decay time $T_2/4 = 11$ ns in optically thin samples or under very low power excitation conditions. In optically thick samples, optical pulse propagation effects (self-induced transparency effects) depend on the separation in time between the first pulse, the second pulse and the echo pulse [16]. Under high-power excitation conditions, this results in decays at low temperature and low concentration which are faster than 11 ns. In fig. 2, the high- and low-concentration crystals have optical densities of 0.35 and 0.48, respectively. The optical density effect results in $\tau_{lc} = 4.5$ ns which is approximately a factor of 2 faster than expected from T_1. This behaviour is consistent with previous experiments [16]. However, the high-concentration crystal, which has a somewhat lower OD than the low-concentration crystal, displays much faster decays. Both τ_f and τ_s are much shorter than τ_{lc}. We compared a wide variety of crystals of high and low concentration with approximately the same ODs, and in each case the high-concentration crystals displayed dramatically faster, non-exponential decays. Additional results presented below demonstrate that the decays are strongly dependent on concentration for fixed OD. Therefore, optical density effects are not responsible for the very fast concentration dependent echo decays observed in these experiments.

The experiments involve a very high degree of excitation ($\pi/2$ and π pulses) of a collection of interacting molecules. Under these conditions, it is possible

for singlet—singlet annihilation to contribute to population relaxation, i.e. two excitations of the system combine to yield a ground state and an excitation of the system at twice the $S_0 \rightarrow S_1$ transition energy. This would produce a non-exponential population decay which is faster than the T_1 measured in a low-concentration experiment. The inset in fig. 2a displays the results of a pump—probe experiment. The pump pulse is a $\pi/2$ pulse to duplicate the initial excitation conditions used in the photon echo experiments. A weak probe pulse is employed. Although the signal-to-noise ratio is not good, the decay is 20 ± 3 ns, which is within experimental error of T_1. Therefore the fast echo decays do not arise from fast population annihilation or other changes in T_1. The fast decays are due to pure dephasing resulting from the concentration dependent delocalization of the excitations.

Fig. 3 displays calculated echo decays for various models of inhomogeneous broadening [14]. Curve A is for a situation in which the inhomogeneous broadening is a Gaussian distribution of excitation energies, and the spatial positions and transition frequencies of molecules are uncorrelated. Curve E is a cal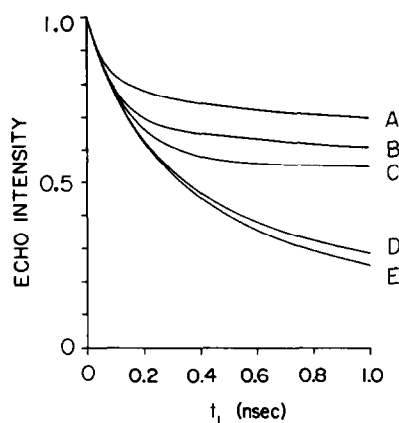culation for a system which is locally homogeneous, i.e molecules which are spatially close together are degenerate. This is the case of complete correlation and results in interacting molecules being degenerate. The other curves are for various degrees of correlation between spatial position and energy. It is clear from this figure that the nature of the local inhomogeneous broadening can have a dramatic influence on the functional form of the time-dependent echo decays.

Curve E in fig. 3 is an exponential decay with T_2 given by eq. (1). Curve A is highly non-exponential. Notice that all curves have the same initial slope, which is determined by eq. (1). The concentration-dependent echo decay curves, such as the one displayed in fig. 2a, qualitatively have the appearance of curve A in fig. 3. There is a fast initial drop followed by a much slower decay. However, quantitative comparison between theory and experiment (discussed further below) demonstrates that the fast component, represented by τ_f, is approximately two orders of magnitude too fast for any reasonable choice of parameters. The LAF theoretical study used a scaling argument to demonstrate that the theoretical treatment of their model is accurate at short time. However the theoretical model does not include the influence of phonons on the system of delocalized states. Scattering among the closely spaced delocalized levels could result in an increased rate of dephasing.

If phonon induced dephasing is responsible for the rapid dephasing at the experimental temperature, 1.5 K, then the photon echo decays should display a very steep temperature dependence. A preliminary study between 1.5 and 2.15 K revealed no change in the echo decays. While this is a small change in T, it is a 40% increase in kT. If temperature effects at 1.5 K were responsible for a two order of magnitude increase in echo decay rate, the 40% increase in T would produce large changes in the signal. Therefore, phonon effects can be ruled out as the cause of the very fast τ_f.

The above considerations lead us to propose that the fast component (τ_f) is not part of the delocalized state photon echo decay. In all samples, it has a time dependence which is similar to the free induction decay (FID) time, i.e. ≈ 20 ps. The free induction decay signal from each beam propagates in the direction of that beam. However, self-diffraction produces a signal in the same direction as the photon echo signal. Self-diffraction is responsible for the "coherence artifacts" encountered in pump—probe experiments. Because of very fast dephasing in a typical room temperature
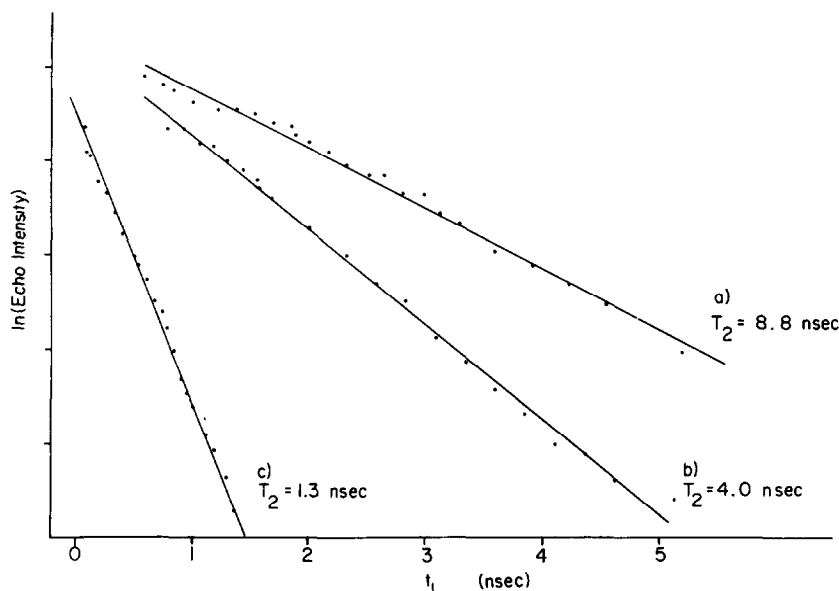

Fig. 3. The photon echo intensity as a function of pulse separation t_1 for various models of inhomogeneous broadening. The homogeneous fwhm is taken to be 1.3 cm^{-1}, the concentration is 1.2×10^{-4} mole PC/mole PTP, and the pulse areas are assumed to be π and $\pi/2$. Curve A corresponds to the situation in which inhomogeneous broadening is a Gaussian distribution of excitation energies, with the spatial positions and transition frequencies of molecules uncorrelated. Curve E corresponds to a system which is locally homogeneous. Curves B, C, and D are for intermediate cases which include varying degrees of correlation between spatial position and transition frequency.

Fig. 4. Photon echo decays ($T_2 = 4\tau$, where τ is the echo decay constant) for three crystals with various concentrations, but similar ODs (0.35–0.6). (a) 1.0×10^{-5} mole PC/mole PTP; (b) 2.9×10^{-5} mole/mole; (c) 8.8×10^{-5} mole/mole. See table 1 for comparison to theory.

solution experiment, the self-diffraction signal is generally faster than the laser pulses. However, in the systems studied here at low temperature with narrow inhomogeneous lines, self-diffraction could arise from the interaction of the long-lived polarization produced by the first pulse with the second pulse, to form a grating [17]. The residual polarization from the first pulse then diffracts from the grating to give a signal in the echo direction. This self-diffraction will decay on the FID timescale rather than on the timescale of the pulse duration. The very thin crystals used in these experiments will enhance the component of the self-diffraction which propagates in the echo direction.

In light of the above discussions, we will consider the true delocalized state photon echo decay to be

the slow component described by the decay time τ_s. Fig. 4 displays the slow component decays for three crystals with various concentrations. In each case the decay is exponential. As the concentration increases, the decay rate increases. Table 1 lists the crystal concentrations, the ODs of the crystals, the decay times measured in these experiments, and the decay times calculated using eq. (1) without adjustable parameters. In eq. (1) $\mu = 1$ D and $a^3 = 3.0 \times 10^{-22}$ cm^3. The agreement between theory and experiment is quite good, particularly in light of the fact that the theory is for a continuum model and that there are experimental uncertainties in both μ and the concentration (f). Notice that the three crystals have approximately the same ODs, again demonstrating that op-

Table 1

Calculated and measured values of T_2 as a function of concentration

	Concentration (mole PC/mole PTP)	OD	T_2 measured (ns) [a]	T_2 calculated (ns) [b]
(a)	1.0×10^{-5}	0.48	8.8	6.3
(b)	2.9×10^{-5}	0.61	4.0	2.2
(c)	8.8×10^{-5}	0.35	1.3	0.7

[a] $T_2 = 4\tau$, where τ is the echo decay constant.   [b] Calculated using eq. (1).

tical density effects [17] are not responsible for the concentration dependence. These results suggest that the system is locally homogeneous and delocalization occurs among a set of essentially degenerate molecules. Theoretical analysis [18] of previous experiments [19] on inorganic crystals indicate that the samples studied were locally inhomogeneous.

4. Concluding remarks

In this paper we have presented experimental observations of the onset of electronic excitation delocalization among a collection of interacting impurity molecules randomly distributed in a host crystal. Optical density effects, population relaxation, and phonon induced dephasing were ruled out as the causes of the fast photon echo decays. It is suggested that the short-time behaviour of the decay is due to self-diffraction involving the polarization induced by the pulses. This polarization, and therefore the self-diffraction, decays on the timescale of the free induction decay.

The electronic excitation delocalization is manifest in the exponential decay of the photon echo signal. The concentration dependent decay times are consistent with theoretical calculations which do not require adjustable parameters. They support a model in which the samples are locally homogeneous, i.e. the interacting molecules (molecules in close proximity to each other) are degenerate. The fast echo decay times (pure dephasing rates) in these samples arise because of the basis nature of the system of delocalized states. Under high-power excitation conditions (large Rabi frequency) used in the photon echo experiments, the dense set of singly excited states are coupled to multiply excited states by the radiation field. The multiple coherences induced in the system of states dephase and produce the rapid echo decays. Thus the photon echo experiment is a direct probe of the nature of the electronic states and the onset and extent of excitation delocalization.

Acknowledgement

References

[1] J. Frenkel, Phys. Rev. 37 (1931) 17, 1276.

[2] Th. Förster, Ann. Physik 2 (1948) 55.

[3] A.S. Davydov, Theory of molecular excitons (Plenum Press, New York, 1971).

[4] D.E. McCumber and M.D. Sturge, J. Appl. Phys. 34 (1963) 1682.

[5] W.H. Hesselink and D.A. Wiersma, J. Chem. Phys. 73 (1980) 648;
L.W. Molenkamp and D.A. Wiersma, J. Chem. Phys. 80 (1984) 3054.

[6] J.L. Skinner, J. Chem. Phys. 77 (1982) 3398.

[7] L. Root and J.L. Skinner, J. Chem. Phys. 81 (1984) 5310.

[8] R.W. Olson, F.G. Patterson, H.W.H. Lee and M.D. Fayer, Chem. Phys. Letters 79 (1981) 403;
H.W.H. Lee, F.G. Patterson, R.W. Olson, D.A. Wiersma and M.D. Fayer, Chem. Phys. Letters 90 (1982) 172;
F.G. Patterson, H.W.H. Lee, W.L. Wilson and M.D. Fayer, Chem. Phys. 84 (1983) 51.

[9] F.G. Patterson, W.L. Wilson, H.W.H. Lee and M.D. Fayer, Chem. Phys. Letters 110 (1984) 7.

[10] J.B.W. Morsink and D.A. Wiersma, Chem. Phys. Letters 89 (1982) 291.

[11] H.W.H. Lee and M.D. Fayer, J. Chem. Phys., to be published.

[12] L. Root and J.L. Skinner, Phys. Rev. B, to be published;
P.W. Anderson, Phys. Rev. 109 (1958) 1492;
J. Klafter and J. Jortner, J. Chem. Phys. 71 (1979) 2210.

[13] W.S. Warren and A.H. Zewail, J. Chem. Phys. 78 (1983) 2298.

[14] R.F. Loring, H.C. Andersen and M.D. Fayer, J. Chem. Phys. 81 (1984) 5395.

[15] R.W. Olson and M.D. Fayer, J. Phys. Chem. 84 (1980) 2001.

[16] R.W. Olson, H.W.H. Lee, F.G. Patterson and M.D. Fayer, J. Chem. Phys. 76 (1982) 31.

[17] T. Yajima and Y. Tiara, J. Phys. Soc. Japan 47 (1979) 1620;
T. Yajima, Y. Ishida and Y. Taira, in: Chemical physics, Vol. 14, ed. F.P. Schäfer (Springer, Berlin, 1980).

[18] L. Root and J.L. Skinner, Phys. Rev. B32 (1985) 4111.

[19] R.M. Shelby and R.M. Macfarlane, Phys. Rev. Letters 45 (1980) 1098;
R.M. Macfarlane and R.M. Shelby, Opt. Commun. 39 (1981) 169.